

Since this is a power series, the total is given by

$$F_{III} = F_3[1 - F_2(1 - F_3)]^{-1} \quad (6)$$

We find for R = H, $F_3 = 0.13$ and $F_{III} = 0.20$, R = Br, $F_3 = 0.13$ and $F_{III} = 0.20$, R = C_6H_5 , $F_3 = 0.13$ and $F_{III} = 0.32$, and R = C_2H_3 , $F_3 = 0.21$ and $F_{III} = 0.41$.

Derivation of Equation 11. Note from Scheme II that

$$K_3 = k_3/k_{-3} = [A^+//T^-]/[A^+][T^-] \approx 2 \times 10^4 M^{-1} \quad (28)$$

$$K_3' = k_3'/k_{-3}' = [A^+//X^-]/[A^+][X^-] \quad (29)$$

$$K_a = k_a/k_{-a} = [TBA^+//T^-]/[TBA^+][T^-] \quad (30)$$

$$K_a' = k_a'/k_{-a}' = [TBA^+//X^-]/[TBA^+][X^-] \approx 3.6 \times 10^4 M^{-1} \quad (31)$$

$$k_X/k_T = [A^+//X^-][TBA^+//T^-]/[A^+//T^-][TBA^+//X^-] = \frac{K_3'}{K_3} \frac{K_a'}{K_a} \quad (32)$$

The rate of reaction from the loose ion pair $[A^+//T^-]$ (steady-state assumption for the intimate ion pair with $k_0 = k_1k_2[k_1 + k_{-2}]^{-1}$) is

$$-\frac{d[A^+]}{dt} = k_0[A^+//T^-] = k_0 \frac{[A^+//T^-]}{[A^+]_0} [A^+]_0 \quad (33)$$

where $[A^+]_0 = [A^+//T^-] + [A^+//X^-] + [A^+]$ is the total concentration

of A^+ present. If only $[A^+//T^-]$ is reactive,

$$k_{II} = k_0 \frac{[A^+//T^-]}{[A^+]_0} \quad (34)$$

At sufficient concentrations of added salt to ensure complete ion pairing of A^+ (i.e., $[A^+] \approx 0$), then $[A^+]_0 = [A^+//T^-]$ when TBAT alone is added, and $[A^+] = [A^+//T^-] + [A^+//X^-]$ when both TBAT and TBAX are added together. Hence,

$$\frac{(k_{II})_T}{(k_{II})_{T+X}} = \frac{k_0}{k_0 \frac{[A^+//T^-]}{[A^+//T^-] + [A^+//X^-]}} = 1 + \frac{[A^+//X^-]}{[A^+//T^-]} \quad (35)$$

For $[TBA^+] \gg [A^+]$, $[TBA^+//T^-] \approx [TBAT]$ added and $[TBA^+//X^-] \approx [TBAX]$ added. Substituting eq 32 into eq 35 yields

$$\frac{(k_{II})_T}{(k_{II})_{T+X}} = 1 + \frac{k_X}{k_T} \frac{[TBAX]}{[TBAT]} \quad (11)$$

Acknowledgment. We thank S. J. Atherton and M. A. J. Rodgers of the Center for Fast Kinetics Research (under support from NIH Grant RR00886 and the University of Texas, Austin) for invaluable help and discussion, A. Levine for technical assistance, and the National Science Foundation and the Robert A. Welch Foundation for financial assistance.

Tailored Excitation for Fourier Transform Ion Cyclotron Resonance Mass Spectrometry

Alan G. Marshall,^{*,†,‡} Tao-Chin Lin Wang,[†] and Tom L. Ricca[‡]

Contribution from the Department of Chemistry, Department of Biochemistry, and Chemical Instrument Center, The Ohio State University, Columbus, Ohio 43210. Received June 3, 1985

Abstract: All present FT/ICR instruments operate with single-pulse or frequency-sweep radio frequency excitation waveforms, which produce excitation power with non-uniform amplitude and limited mass selectivity. This paper introduces a general "tailored" excitation time-domain waveform obtained by inverse Fourier transformation of the desired excitation spectrum. The new method includes all other excitation waveforms as subsets and may be operated in direct or heterodyne mode. Major applications include the following: flatter excitation power over the detected mass range, excitation power with one or more windows for suppression of large peaks or for more selective ion ejection for MS/MS, and multiple-ion monitoring with simultaneous detection of any number of selected mass-to-charge ratios. Theoretical and experimental examples of all three types of excitation are given. The method is readily adapted to existing instruments with minor hardware and software modifications.

Since its introduction in 1974,^{1,2} Fourier transform ion cyclotron resonance mass spectrometry has advanced to become an extraordinarily versatile mass spectrometric technique whose advantages have recently been reviewed.^{3,4} Briefly, its most important features are the following: simultaneous detection of the entire mass spectrum at once (typically in ca. 0.1 s); potentially ultrahigh mass resolution (e.g., 1000000:1 at mass-to-charge ratio, m/z 200); and an upper mass limit that has yet to be reached. Although major progress has been made in improving FT/ICR detection (e.g., reducing base pressure to about 10^{-10} torr, extending the bandwidth of the detection circuit, shielding of the transmitter and detector leads, differentially-pumped dual-cell,⁵ etc.), there have been no fundamental advances in FT/ICR excitation since 1974.

Ideal FT/ICR excitation power spectra (i.e., excitation magnitude as a function of frequency) are shown in Figure 1. For ordinary detection, one might choose perfectly flat excitation power

(Figure 1, top trace), in order to excite ions of various m/z values to a common orbital radius,⁶ to yield a mass spectrum in which the intensities (areas) of the various peaks accurately reflect the relative numbers of ions at those m/z values.⁷ The excitation spectrum shown in the middle trace of Figure 1 consists of flat power over a specified mass range, with a zero-power window of specifiable width. Windowed excitation is useful for suppressing (by failing to excite) a large peak whose presence could make detection of small peaks difficult. Windowed excitation may also be used to eject ions of all but one m/z value; ions at that m/z

(1) Comisarow, M. B.; Marshall, A. G. *Chem. Phys. Lett.* **1974**, *25*, 282-283.

(2) Comisarow, M. B.; Marshall, A. G. *Chem. Phys. Lett.* **1974**, *26*, 489-490.

(3) Marshall, A. G. *Acc. Chem. Res.* **1985**, *18*, 316-322.

(4) Wanczek, K. P. *Int. J. Mass Spectrom. Ion Proc.* **1984**, *60*, 11-60.

Gross, M. L.; Rempel, D. L. *Science* **1984**, *226*, 261-268.

(5) Ghaderi, S.; Littlejohn, D. P. 1985 33rd American Society for Mass Spectrometry Annual Conference, San Diego, CA, May, 1985, Paper No. ROC12.

(6) Comisarow, M. B. *J. Chem. Phys.* **1978**, *69*, 4097; see also ref 12.

(7) Comisarow, M. B. *J. Chem. Phys.* **1978**, *69*, 4097-4104.

[†]Department of Chemistry.

[‡]Department of Biochemistry.

[‡]Chemical Instrument Center.

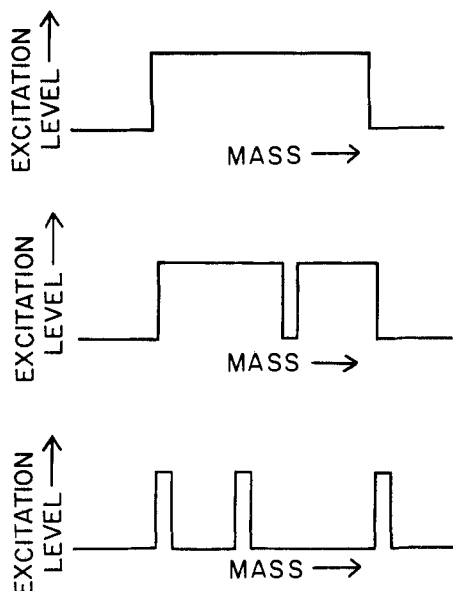


Figure 1. Desired excitation power spectra for Fourier transform ion cyclotron resonance mass spectrometry (FT/ICR). Top: Flat power over a specified mass range, for ordinary detection and/or isotope-ratio measurements. Middle: Flat excitation with a zero-power window, for use in the first stage of MS/MS experiments. Bottom: Multiple-frequency excitation for use in multiple-ion monitoring.

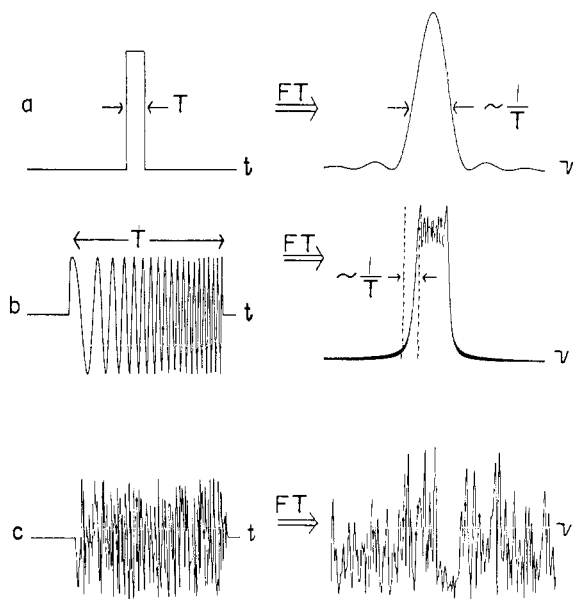


Figure 2. Previously employed time-domain excitation waveforms and their corresponding frequency-domain magnitude-mode spectra. Top: Single-pulse excitation (1). Middle: Frequency-sweep excitation (2, 12). Bottom: Pseudorandom noise excitation (13). Note the nonflat power and broad cutoff shoulders.

value may subsequently be excited and induced (by a pulse of collision gas⁸ or laser⁹) to fragment, providing MS/MS capability¹⁰ with a single spectrometer. Finally, the excitation shown as the bottom trace of Figure 1 could be used for selective ion monitoring, to detect any number of specified m/z values simultaneously.

Currently available time-domain excitation waveforms and their corresponding frequency-domain magnitude spectra are shown in Figure 2. Single-pulse excitation (top trace of Figure 2) was the method used to produce the first Fourier transform mass

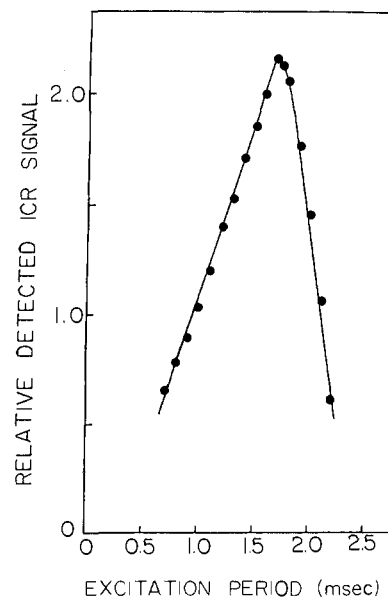


Figure 3. Detected FT/ICR signal intensity as a function of excitation period with constant-amplitude, constant-phase, single-frequency time-domain excitation.

spectrum (1), and it is still the principal excitation waveform in Fourier transform nuclear magnetic resonance (FT/NMR) spectrometry. Although the single-pulse excitation magnitude spectrum is far from flat, it is nearly flat over a bandwidth of about $\pm(0.1/T)$ Hz, where T is the duration of the time-domain pulse. In FT/NMR, a typical spectral detection bandwidth might be ca. 10000 Hz; thus, a pulse of a few microsec duration can produce satisfactorily flat excitation power across the spectral range of interest. However, for fixed magnetic field strength, $B = 3$ T, ion cyclotron resonance frequency, ν , varies from about 2.6 MHz

$$\nu = \frac{zB}{2\pi m} \text{ (mks units)} \quad (1)$$

at m/z 18 (e.g., H_2O^+) to about 50 kHz at m/z 1000. As noted qualitatively by Comisarow¹¹ and quantitatively by Marshall,¹² the ca. 2 MHz bandwidths of the full mass range FT/ICR experiment would require a single-pulse excitation of duration ca. 0.1 μs and unreasonably large amplitude (ca. 10^4 V). Single-pulse excitation is therefore feasible only for excitation or ejection of ions within a very narrow m/z range.

In order to extend the excitation bandwidth without the need for high excitation power, Comisarow proposed the frequency-sweep excitation shown as the middle trace in Figure 2. It achieved the desired bandwidth² and is the excitation method now in use in all (ca. 35) current FT/ICR instruments. However, Figure 2 shows that the frequency-sweep excitation power is markedly non-uniform in amplitude. The power spectrum may be made flatter¹² but only by slowing the frequency sweep so much that the ICR signal will be lost (due to loss of coherence in ICR motion because of ion-molecule collisions or imperfect electric fields in the detector cell) by the time the excitation period is over.

Finally, pseudorandom noise may be used as a spectral source.¹³ However, the power spectrum for noise excitation is even more non-uniform than for a frequency-sweep, even when based on maximal-length shift register sequences.

A new and much more general class of excitation waveforms is possible, provided that the system is "linear", i.e., that the amplitude of the response is linearly proportional to the amplitude of the excitation. We recently demonstrated¹⁴ that ICR excita-

(8) Cody, R. B.; Freiser, B. S. *Int. J. Mass Spectrom. Ion Phys.* **1982**, *41*, 199.

(9) Dünbar, R. C. "Gas Phase Ion Chemistry"; Bowers, M. T., Ed.; Academic Press: New York, 1979; Vol. II, Chapter 14 (1984; Chapter 20).

(10) McLafferty, F. W. *Science* **1981**, *214*, 280-287.

(11) Comisarow, M. B., private communication, 1973.

(12) Marshall, A. G.; Roe, D. C. *J. Chem. Phys.* **1980**, *73*, 1581-1590.

(13) Marshall, A. G.; Wang, T.-C. L.; Ricca, T. L. *Chem. Phys. Lett.* **1984**, *108*, 63-66.

(14) Marshall, A. G.; Wang, T.-C. L.; Ricca, T. L. *Chem. Phys. Lett.* **1984**, *105*, 233-236.

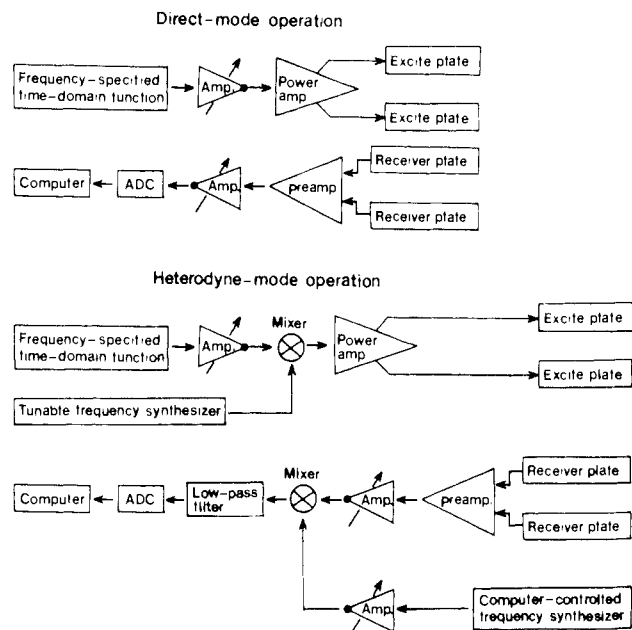


Figure 4. Block diagrams for direct-mode (top) and heterodyne-mode (bottom) tailored excitation (see text).

tion/detection in a cubic trapped-ion cell¹⁵ is indeed linear. Figure 3 (circles) shows that the ICR signal detected for the $C_9F_{20}N^+$ electron ionization fragment of perfluorotributylamine increases linearly as the length of the single-pulse excitation period, until ions are driven to such large-radius orbits that the signal is lost.

For a linear ICR system, one need not determine the trajectories of individual ions in order to compute the ICR response; since the response is proportional to the excitation, it suffices to determine the excitation magnitude spectrum obtained by Fourier transformation of the time-domain excitation waveform. Therefore, we propose a "tailored" excitation method, in which virtually any desired excitation spectrum is specified in the frequency domain, and the corresponding time-domain excitation waveform is then generated by Fourier transformation of that spectrum.

Experimental Section

All theoretical waveforms and experimental spectra were produced with a modified Nicolet FTMS-1000 spectrometer. In order to institute a tailored excitation with minimal software and hardware modifications, the Nicolet 1280 computer was first used to specify a frequency-domain excitation spectrum, by using the existing software commands that were originally designed to specify double-resonance windows. An inverse FT then generated a 4K time-domain excitation waveform, which was stored in an unused part of core memory. Next, it is necessary to know that during normal frequency-sweep excitation, the FTMS-1000 constructs the time-domain excitation waveform by repeatedly stepping through a 4K-word look-up memory which contains one-fourth of a digitized sine wave. Therefore, in order to generate the desired excitation waveform, the computer was programmed for single-frequency excitation for a total excitation period chosen to correspond to one-fourth of one cycle of that excitation frequency, so that there is just enough time to sweep once through the computer's sine-wave look-up table. However, the look-up table location was switched to correspond to the desired time-domain excitation data set.

In direct-mode operation (see Figure 4), frequencies are synthesized directly—i.e., the frequency spectrum ranges from zero to the highest specified frequency (lowest specified mass), and the digitized output of the look-up memory is fed at a clocked rate to a digital-to-analog converter, and then to the excitation power amplifier and thence to the transmitter plates of the cell. Direct-mode operation has the advantage that all remaining instrumental parameters may be specified just as for frequency-sweep operation. However, direct-mode synthesis presents the obvious problem that only limited excitation frequency resolution (and thus mass resolution) is available, since the whole frequency range must be digitized with a limited number (say, 4096) of data points.

Much improved resolution in the excitation spectrum is made possible by heterodyne-mode synthesis (see Figure 4), in which a narrow band of frequencies ranging from (say) 0 to 20 kHz is synthesized and stored in

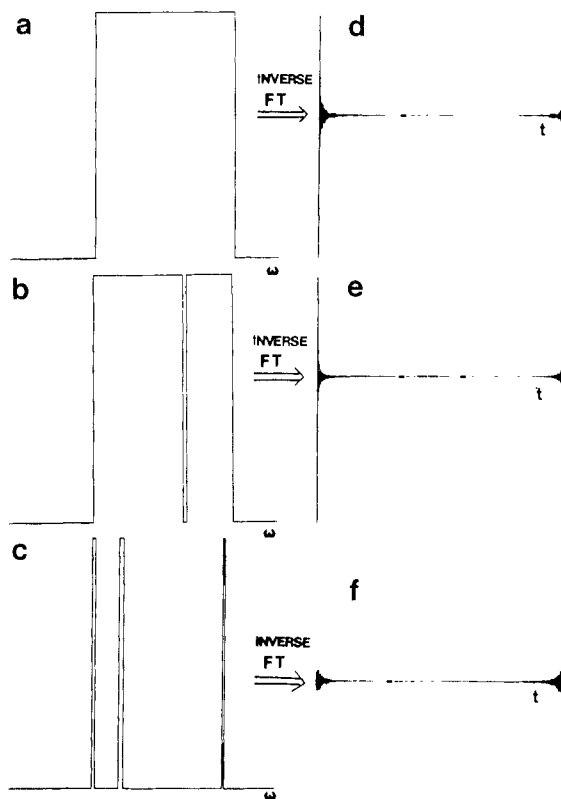


Figure 5. Time-domain excitation waveforms (right) generated by inverse Fourier transformation of the desired frequency-domain excitation spectra (left). Because mass and frequency are inversely related in ICR, the desired excitation mass spectra of Figure 1 are readily converted to those shown at the left in this figure.

the look-up table, clocked out at a suitably slow rate, digital-to-analog converted, mixed with a high-frequency radio frequency carrier signal centered at the frequency band of interest, and then sent to the transmitter power amplifier and transmitter plates. After the transmitter is turned off, the detected ICR signal from the receiver plates is amplified and heterodyned in the usual way against a second reference radio frequency signal, before digitization and Fourier transformation to give the final FT/ICR ion mass spectrum.

The excitation waveforms to be discussed in Figure 5 require substantially higher excitation amplitude than a frequency-sweep of the same frequency-domain bandwidth (see Results and Discussion). Therefore, it was necessary to construct a transmitter power amplifier with about 20 dB higher gain than for frequency-sweep mode. No increase in transmitter gain was required for phase-scrambled tailored excitation (see Discussion).

Results and Discussion

Tailored Excitation. The basic principle of tailored excitation is shown in Figure 5. The desired mass-domain excitation profile (Figure 1) is converted via eq 1 to the corresponding frequency-domain excitation spectrum (Figure 5 a–c). An inverse Fourier transform then produces the time-domain excitation waveform (Figure 5 d–f) for the desired mass-domain excitation.

The large dynamic range exhibited in waveforms d and e in Figure 5, and seen more clearly in Figure 6b, presents several related practical problems. First, because most of the excitation power is concentrated into a small fraction of the time-domain excitation period, the excitation amplitude must be much larger (e.g., about a factor of 10) than for frequency-sweep excitation with its approximately constant time-domain peak-to-peak amplitude. Second, the computer word length (20 bits for the Nicolet 1280 computer) limits the digital dynamic range, both for data storage and computations. Third, the high dynamic range in the transmitter circuitry poses severe tests for linearity and transient analog response. For all of these reasons, it is perhaps not surprising to find that the actual excitation power produced at the transmitter plates is substantially less uniform than in the originally specified waveform (see Figure 7b).

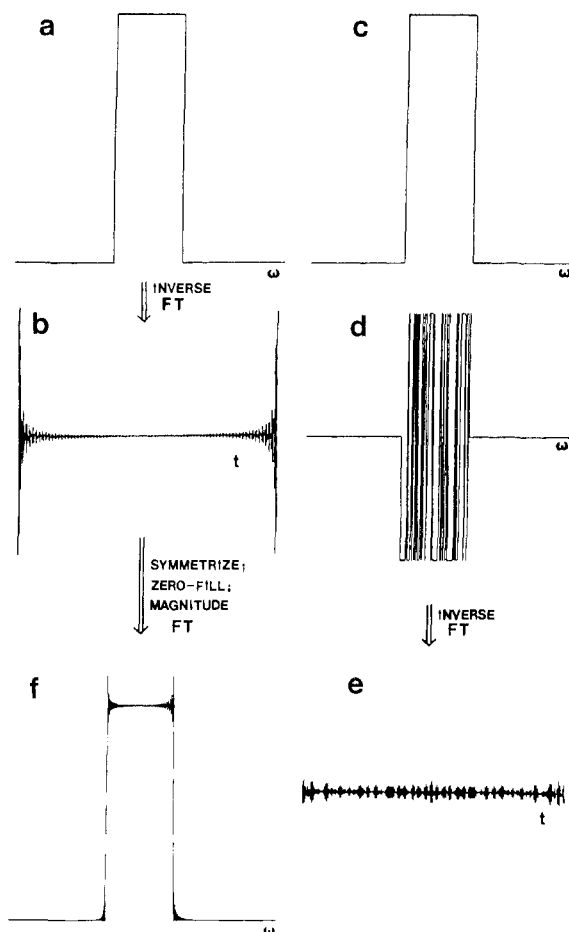


Figure 6. Effect of frequency-domain phase scrambling upon time-domain excitation waveforms. A constant-phase excitation spectrum (a) when subjected directly to Fourier transformation yields a time-domain waveform (b) exhibiting high dynamic range and requiring high excitation power because the time signal is so small during most of the excitation period. However, when the same excitation spectrum is first phase scrambled (d) by multiplying the points by a pseudorandom sequence of +1 and -1, subsequent Fourier transformation gives a time-domain waveform (e) with greatly reduced dynamic range and roughly constant time-domain amplitude (and thus much lower required excitation power). Spectrum f is the Fourier transform of symmetrized, zero-filled (b), as discussed in the text.

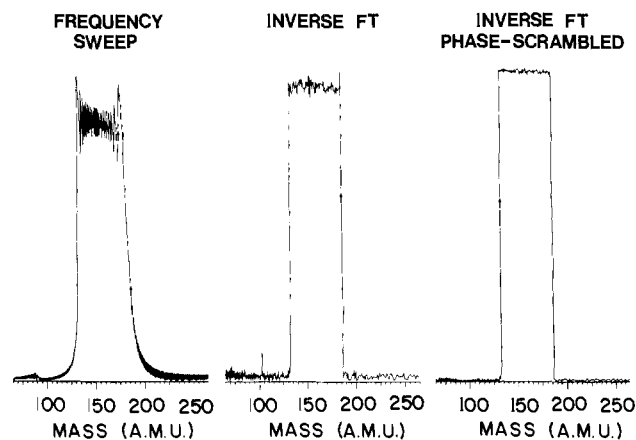


Figure 7. Magnitude-mode excitation spectra. Left: Time-domain frequency-sweep (1 ms). Middle: Constant-phase inverse-FT waveform (1.024 ms) shown as Figure 6b. Right: phase-scrambled inverse-FT waveform (1.024 ms) shown as Figure 6d. Note the flatter excitation power obtained by the tailored excitation.

Phase Scrambling. The high dynamic range in (for example) the time-domain waveform of Figure 6b results from the common phase relation between all of the frequency-domain excitation

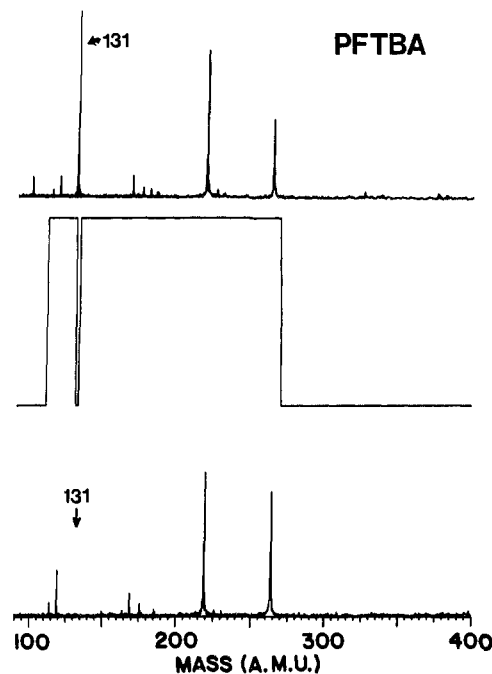


Figure 8. FT/ICR spectra obtained via frequency-sweep (top) and windowed (bottom) FT/ICR direct-mode tailored excitation for perfluorotributylamine, obtained via 1.024 ms direct-mode frequency synthesis (middle). Note that the large peak at m/z 131 observed with frequency-sweep excitation is absent when a zero-power window from $130 < m/z < 132$ is introduced.

spectral components—namely, zero-phase (i.e., pure cosine) at each frequency. Thus, there is a sharp maximum in the time-domain signal at time zero, much as for the NMR free-induction decay or the centerburst in an FT/IR interferogram,¹⁶ because cosines at all frequencies start out as maxima at time zero. Recognizing the origin of the problem leads at once to a solution—namely, “scrambling” the frequency-domain phases in a pseudorandom way, so that the phase coherence of the spectral components is destroyed.¹⁷ For example, a frequency-domain flat-power spectrum (Figure 6c) can be multiplied, point by point, by a pseudorandom sequence consisting of +1 and -1 to give the spectrum shown in Figure 6d. It is important to appreciate that both spectra (c and d in Figure 6) have the same power spectrum (namely, perfectly rectangular); it is just that the phases of the frequency components are equal in Figure 6c but scrambled in Figure 6d. Finally, an inverse FT of the spectrum in Figure 6d yields a time-domain excitation waveform (Figure 6e) with approximately constant power throughout the excitation period; thus, the aforementioned dynamic range difficulties do not arise.

Inspection of parts d–f in Figure 5 suggests that phase-scrambling will be most necessary for very simple excitation spectra, for which the time-domain dynamic range problem would otherwise be especially severe. In practice, we find that the nature of the pseudorandom sequence does not appear to be critical. Figure 6d was produced by the “RND” random-number generator command from Basic.

Figure 7 compares experimentally detected magnitude spectra of the excitation, for frequency-sweep, constant-phase tailored excitation, and phase-scrambled tailored excitation, all for the same time-domain excitation period. The phase-scrambled result offers clearly improved uniformity in amplitude over the specified mass range. Experimental phase-scrambled tailored excitation applications will now be presented.

Direct-Mode Windowed Excitation. Figure 8 shows the FT/ICR experimental magnitude-mode response spectra, produced

(15) Comisarow, M. B. *Int. J. Mass Spectrom. Ion Phys.* **1981**, *37*, 241–257.

(16) Marshall, A. G. “Physical Methods in Modern Chemical Analysis”; Kuwana, T., Ed.; Academic Press: New York, 1983; Vol. 3, pp 57–135.

(17) Tomlinson, B. L.; Hill, H. D. W. *J. Chem. Phys.* **1973**, *59*, 1775.

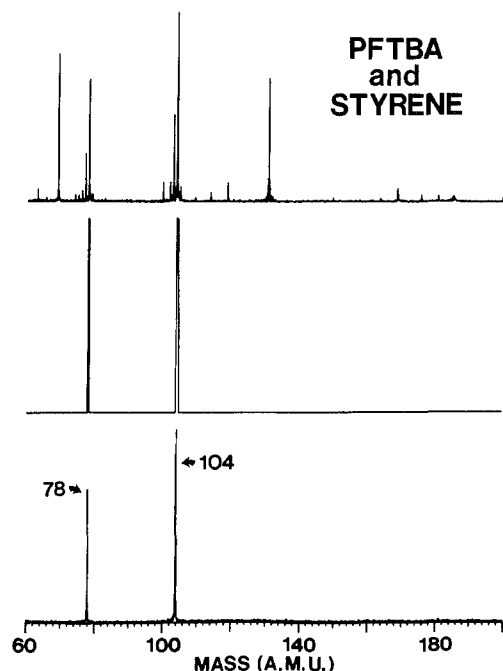


Figure 9. Multiple-ion monitoring via tailored FT/ICR excitation, obtained via direct-mode frequency synthesis. Top: Response spectrum from frequency-sweep excitation (1 ms). Middle: Excitation spectrum of tailored waveform (1.024 ms) itself, with non-zero power only at the two frequencies corresponding to m/z 78 and 104. Bottom: FT/ICR response spectrum from the above excitation. Note that m/z 104 is clearly visible without contamination from m/z 103 or 105.

by frequency-sweep (top spectrum) and windowed excitation (bottom spectrum), for perfluorotributylamine. The strong peak at m/z 131 is completely suppressed by use of excitation with a zero-power window extending from $130 < m/z < 132$. The m/z 131 ions are still present—it is just that their thermal velocity produces such small (and incoherent) ICR orbits that no signal is visible.

Windowed direct-mode excitation (and its heterodyne analog—see below) should prove important in increasing the dynamic range for FT/ICR, because windowed excitation may be used to eliminate large peaks and therefore facilitate the detection and quantitation of small peaks. Another application for windowed excitation is mass spectrometry/mass spectrometry, in which all but one narrowly selected m/z range can be ejected, leaving a single isotopic peak for further fragmentation study.

Direct-Mode Multiple-Ion Monitoring. Figure 9 shows a two-ion simultaneous monitoring example, based on direct-mode tailored excitation. In this example, frequency-sweep excitation of an ionized mixture of perfluorotributylamine and styrene yields one group of three adjacent peaks at m/z 77, 78, and 79, and another three adjacent peaks at m/z 103, 104, and 105. However, selected-ion excitation at m/z 78 and 104 extracts those two peaks, without contamination from m/z 77, 79, 103, or 105. An important feature is that both m/z values are excited simultaneously and detected simultaneously—a capability of obvious value in real-time monitoring of flow systems—and not found in any other mass spectrometer design. Another advantage is that the ion selectivity can be modified with software changes only; no hardware modifications are needed to change from one set of monitored m/z values to another. Even more selective monitoring is possible with the heterodyne mode (see below).

Heterodyne-Mode Windowed Excitation. The ultimate selectivity for tailored excitation is reached with heterodyne-mode operation. For example, Figure 10 demonstrates heterodyne-mode windowed excitation with a frequency-domain window of 1 kHz (corresponding to a mass selectivity < 0.02 amu). The performance demonstrated in Figures 8–10 could be improved by the following:

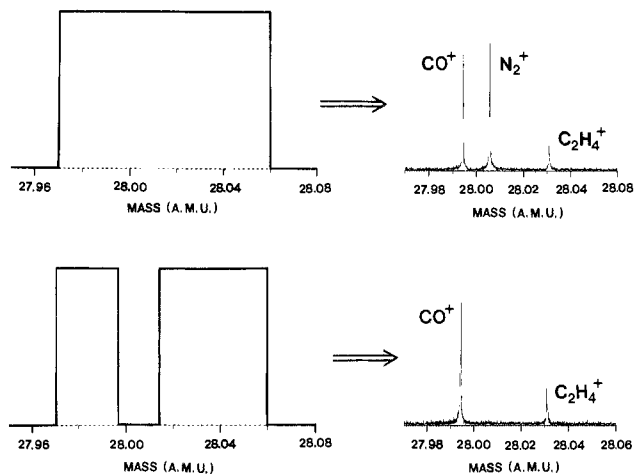


Figure 10. Flat (top left) and windowed (bottom left) FT/ICR excitation for a mixture of CO^+ , N_2^+ , and C_2H_4^+ , obtained via heterodyne-mode frequency synthesis (4.096 ms). In the FT/ICR response spectrum, all three signals are visible with flat excitation (upper right), whereas the N_2^+ signal is absent from the windowed excitation, because no power was applied at the ICR frequency for N_2^+ . Heterodyne-mode excitation provides much higher mass resolution (ca. 0.01 amu selectivity in this case) in the excitation spectrum (compare to Figure 9).

longer word length and/or floating point arithmetic to avoid computation errors in the various forward and inverse FT manipulations; longer excitation period to increase analog resolution; and larger excitation waveform data sets ($\geq 64\text{K}$) to increase digital resolution in the excitation spectrum.

When the time-domain excitation waveform is symmetrized (to make it an even function), zero-filled (to increase the digital resolution in the frequency-domain), and Fourier transformed, the resultant magnitude-mode spectrum (Figure 6f) shows the auxiliary “wiggles” (at spacing of ca. $1/T$ Hz) that must result from truncating any time-domain signal after T s (in this case, 1 ms). However, it is important to recognize that for time-shared detection (see below), the detected spectrum is sampled at the zero-crossings of the “wiggles” (unlike the frequency-sweep case); thus, the magnitude-mode spectra shown in Figure 7 should be realized experimentally with time-shared excitation/detection. Even when excitation and detection are temporally separated, the “wiggles” for tailored excitation will be less pronounced than for frequency-sweep excitation, according to the number of times the frequency-sweep must be interrupted in order to generate the desired excitation peaks and/or windows.

Stochastic Excitation/Detection. Because the frequency-domain peak separation at constant magnetic field in ICR varies inversely with mass (see eq 1), comparable mass selectivity (in the *excitation*) at different m/z requires an excitation period which is proportional to m/z . Thus, at high m/z , for which mass resolution corresponding to a frequency resolution of ≤ 10 Hz might be required, the excitation period could be 100 ms or more. At typical operating pressure (ca. 10^{-8} torr), much of the time-domain ICR response signal will have decayed (due to ion-molecule collisions) during that period. However, if the excitation and detection are time-shared (much as with gated decoupling in FT/NMR), then the excitation period can be made as long as the detection period, and mass resolution can be made as high for the excitation as for the detection. We designate time-shared tailored excitation (direct-mode or heterodyne-mode) as “stochastic” FT/ICR/MS and will report separately on its implementation.¹⁸

Acknowledgment. This work was supported by grants (to A.G.M.) from the U.S.A. Public Health Service (N.I.H. GM-31683) and The Ohio State University.